Pos'a: 79789

Metallic Copper Colloids by Laser Ablation of Non Metallic Copper Precursor Suspensions

Christian A. Schaumberg,[†] Markus Wollgarten,[‡] and Klaus Rademann[*,†]

Department of Chemistry, Humboldt-Universität zu Berlin, Brook-Taylor-Straße 2, 12489 Berlin, Germany, and Helmholtz-Zentrum Berlin für Materialien und Energie GmbH, Hahn-Meitner-Platz 1, 14109 Berlin, Germany

E-mail: klaus.rademann@chemie.hu-berlin.de

Phone: +49 (0)30 2093 5565. Fax: +49 (0)30 2093 5559

*To whom correspondence should be addressed
[†]Humboldt-Universität zu Berlin
[‡]Helmholtz-Zentrum Berlin

Abstract

Pulsed laser ablation in liquids (PLAL) has developed to a convenient and efficient method for the synthesis of colloidal solutions. So far, in most cases the laser pulse is focused on bulk targets like metal plates. An interesting alternative is the usage of suspended precursors. This leads to higher production rates and simpler setups. A thorough understanding of the mechanism is essential in order to gain control over the characteristics of the synthesized nanoparticles. Therefore, we investigated the formation of copper colloids by PLAL of CuO, Cu_3N, $Cu(N_3)_2$ and Cu_2C_2 powders in organic liquids. Thus we can compare copper precursors based on elements of the 4^{th}, 5^{th}, and 6^{th} main group. The chemical composition of the resulting nanoparticles is revealed by electron energy loss spectroscopy (EELS).

Keywords

Pulsed Laser Ablation in Liquids, Copper Colloids, Electron Energy Loss Spectroscopy, Energy Filtered Transmission Electron Microscopy

Introduction

Since the dust of nanoparticles is considered being hazardous, the handling of nanoparticles has become a major issue.[1] A quite convenient approach to circumvent this issue is the use of colloidal solutions. Here the nanoparticles are emerged in a suitable liquid and therefore can be handled like chemical solutions. There are several approaches to the synthesis of stable colloids. Herein the wet chemical synthesis of metal colloids is the most prominent one.[2,3] The major drawback of the wet chemical approach is the need for reducing agents and stabilizers. Several applications need "pure" colloids. In case of medical treatments for example toxic additives can not be tolerated.[4–6] The surfactants used to control the growth process and stabilizing the colloid may also compete for active sites when nanoparticles are

used as catalysts.[7] Surfactants may also hinder the deposition of a catalyst on a support.[8] Another interesting field for nanotechnology is the design of improved thermoelectric devices. The efficiency of a thermoelectric material at a given temperature T is represented by its figure of merit: $zT = \sigma\kappa^{-1}TS^2$. While the Seebeck coefficient S is fixed for a certain material, the figure of merit can be improved by lowering the thermal conductivity κ while the electrical conductivity σ is intended to be unchanged. The usage of nanostructured materials may lead to an increased scattering of phonons at the grain boundaries. Thus the thermal conductivity is lowered while the electrical conductivity is less affected.[9] Remaining reducing agents and stabilizers may thwart any improvements of ZT by drastically reducing the electrical conductivity σ if such materials are prepared from a colloidal solution.

One method to bypass these medical, catalytic, and thermoelectric issues is the utilization of pulsed laser ablation in liquids (PLAL).[10–12] The typical approach for PLAL is to focus a pulsed laser on the surface of a solid target (e.g. a metal plate or a metal rod) which is immersed in a liquid.[13,14] This approach was already successfully applied to a wide range of materials.[15] A promising alternative to bulk targets are suspensions. Here, a μm powder is suspended in a liquid during the ablation.[16] Although this approach provides some advantages and opportunities, it is so far quite unheeded. While the ablation of bulk targets requires a carefully set focus, the ablation of suspensions is less demanding at this point. As long as the necessary intensity is reached in some place of the suspension, the exact setting of the focus is less crucial and even unfocused beams may be used. Another major issue of all PLAL experiments is the reachable production rate. As the actual experimental settings have an important influence, the comparison of production rates from bulk targets and suspensions is challenging. Though, for similar laser powers the ablation of suspensions show higher production rates.[11,12]

For the synthesis of metal colloids by PLAL of bulk targets mostly pure metal plates are used. Thus no chemical changes occur. This is quite different when using suspensions. PLAL of CuO powders lead to Cu colloids.[16,17] Ag colloids may be obtained from Ag_2O

powders.[18] This leads to some important consequences. The chemical composition of the resulting nanoparticles may not be identical to the used target material although this is often assumed in the literature.[19,20]

In order to design a suitable synthesis route for a certain material a detailed knowledge of the mechanisms is mandatory. Several investigations provide mechanistic concepts for the synthesis of colloids by laser ablation in general and the PLAL of bulk targets in particular.[21–23] Furthermore, many mechanistic studies cover the fragmentation and site reduction of pre-synthesized colloids. Here, photothermal surface evaporation,[24] coulomb explosions[25] and near-field ablation[26] are considered to be the most relevant mechanisms. So far, there are few investigations whether these concepts are also valid for the PLAL of suspensions of μm powders. Most publications treat the PLAL of suspensions as a simple fragmentation.[17] Keeping in mind that often the chemical composition changes during the ablation, the exact mechanism is likely to be more complex. More detailed studies discuss, in addition to the fragmentation, a coalescence mechanism.[27] This still not explains the observed redox reaction for the ablation of CuO and Ag_2O powders.[17,28] Further studies focus on the chemical processes during the laser ablation.[29]

Therefore, the aim of this work is to investigate the chemical processes during the formation of copper colloids. Copper colloids are suitable model systems for two reasons. On the one hand, the formation and aging of copper nanoparticles can be monitored by UV-Vis spectroscopy due to their surface plasmon resonance.[30] On the other hand, the different oxidation states can be distinguished by electron energy loss spectroscopy of the copper $L_{2,3}$ edges.[31,32] Transition metals show so called "white lines" in EELS, i.e. narrow band of transition energies (ΔE approx. 1-2 eV). These appear as a result of an electron transition from a p orbital to an unoccupied d orbital. If the d orbitals are fully occupied, these white lines are suppressed as it is observed for copper in the oxidation state zero. Our investigations are based on the established synthesis of copper colloids by PLAL of CuO powders suspended in organic liquids. In addition, we evaluate the opportunities offered by alternative precursors

like Cu_3N, $Cu(N_3)_2$ and Cu_2C_2 for the first time.

This article is structured by discussing the different precursors. After a brief description of the experimental procedure, the first section deals with the well established laser ablation of CuO suspensions. The second section describes the impact of the results of the usage of Cu_3N on the understanding of the mechanism. The subsequent discussion on the ablation of high energetic materials like $Cu(N_3)_2$ reveals the capabilities of optimizing the production rates by designing new precursors. Finally, the laser ablation of Cu_2C_2 shows that the formation mechanism can be manipulated in order to synthesize colloids with desired properties.

Experimental

The laser ablation was realized with a q switched Nd:YAG laser Ultra (Quantel, France). The 1^{st} (532 nm, 45 mJ/pulse, 6 ns), 2^{nd} (355 nm, 20 mJ/pulse, 5 ns) and 3^{rd} (266 nm, 15 mJ/pulse, 5 ns) harmonic were used. The laser beam was not further focused, resulting in a beam diameter of approximately 3 mm. Acetone (99.8%, Carl Roth), ethyl acetate (99.5%, Carl Roth), acetonitrile (99.9%, Carl Roth), copper(II) oxide (99.5%, mesh 200, Strem Chemicals) and copper(I) nitride (99.5%, mesh 200, Alfa Aesar) were used as received.

Copper(II) azide was synthesized by an optimized route following Straumanis and Cīrulis.[33] Copper(II) bromide (100 mg, 98%, Merck) is dissolved in ethanol (10 ml, 99.8%, Carl Roth). Sodium azide (50 mg, 99%, Carl Roth) is added and the solution is stirred until the NaN_3 is completely dissolved. As the sodium azide dissolves, copper(II) azide is formed as a black/dark green precipitate. After 2 hours, the precipitate is filtered and subsequently washed with ethanol and ethyl acetate. Warning: The authors strongly recommend not to exceed the quantities given above and to handle the precipitate with care as dry $Cu(N_3)_2$ is highly explosive!

Copper(I) acetylide was synthesized as follows: Copper(I) chloride (250 mg, 97%, Carl Roth) is solved in aqueous ammonia solution (25 ml, 25%, Carl Roth). The solution is

cooled to 0 °C. A reddish precipitate of copper(I) acetylide is formed when ethyne is passed through this solution. The precipitate is immediately filtered and subsequently washed with cold water, ethanol and ethyl acetate.

The following procedure was applied for the PLAL of suspensions: 3 - 10 mg (0.1 mmol Cu) of the copper precursor is suspended in 7.8 ml of an organic liquid. The used poly propylene vessel is closed by a glass slide. The laser beam enters the reaction vessel from the top through the glass slide. The suspension is vigorously stirred during the ablation. The suspension is ablated for 10 s - 10 min with 20 Hz resulting in 200 to 12000 laser pulses.

The UV-Vis spectra were taken with an USB2000 or HR2000 detector (OceanOptics, U.S.A.), a SL5-DH deuterium-halogen lamp (StellarNet, U.S.A.) and fiber optics.

Transmission electron microscopy (TEM) images, energy filtered transmission electron microscopy (EFTEM) images and electron energy loss spectra (EELS) were recorded with a Libra 200FE TEM (Zeiss, Germany) equipped with a ultrascan CCD camera (Gatan, U.S.A.). The accelerating voltage was set to 200 kV for all measurements. For conventional TEM images, an energy selecting slit was placed at the exit of the in-column filter to exclude electrons, which suffered inelastic scattering (zero loss filtered (ZLF) images). EFTEM images were taken with an automated routine providing spatial drift corrections.[34] EELS data were collected with a circular aperture equivalent to a sample area with a diameter of 125 nm. A 4-fold hardware binning was applied during recording. Up to 10 spectra were accumulated at different areas of the CCD in order to improve the signal to noise ratio and avoid artifacts. The EEL spectra are background corrected by subtraction of a power law function fitted to the pre-edge region. The samples were prepared by dropping the colloid on a carbon coated copper grid CF200-Cu (Electron Microscopy Sciences, U.S.A.) or a silicon nitride membrane DuraSiN (Electron Microscopy Sciences, U.S.A.).

The quantification of the copper content of the generated colloids was performed by flame atomic absorption spectrometry. In order to avoid an overestimation through unreacted precursor powder, all samples were allowed to sediment for one hour. An aliquot of the

supernatant colloid was heated until the organic solvent was completely evaporated. The sample was dissolved in concentrated nitric acid at elevated temperatures. After dilution with deionized water the copper content was measured with an AAnalyst 200 (PerkinElmer, U.S.A.).

Results and discussion

The pulsed laser ablation of copper(II) oxide powder suspended in an organic liquid was first reported by Yeh et al. using iso-propanol as liquid.[16] For this work, the synthesis was performed in ethyl acetate to enhance the colloidal stability. We investigated the possible use of different copper precursors. Table 1 lists all tested precursors. Interestingly, the PLAL is

Table 1: Tested precursors for the laser ablation of suspended precursors

precursor	resulting colloid
Cu	-
Cu_2O	-
CuO	deep red
Cu_2S	-
CuS	pale yellow solution
Cu_3N	turbid, black / green
$Cu(N_3)_2$	turbid, black
Cu_2C_2	black / brown
$Cu(Ac)_2$	-
$Cu(acac)_2$	-
$CuSO_4$	-
$CuCO_3$	-

not possible with metallic copper powder or copper(I) oxide with the given setup. This leads to the conclusion that the threshold for the laser ablation of these materials is significantly higher as compared to copper(II) oxide. As high laser fluences are not always desirable, a proper choice of the precursor is crucial. In the following, we present the successful generation of copper colloids via PLAL of CuO, Cu_3N, $Cu(N_3)_2$ and Cu_2C_2.

Copper(II) oxide

The laser ablation of CuO in ethyl acetate leads to deep red solutions. Within a few hours the color changes to green. This phenomenon was investigated by UV-Vis spectroscopy. Figure 1 shows the UV-Vis spectra 2 to 6 hours after the synthesis. The spectra exhibit features of a surface plasmon resonance. This indicates the presence of metallic nanoparticles. During

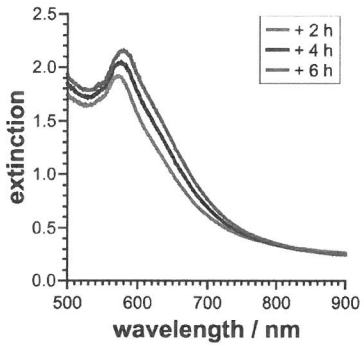

Figure 1: UV-Vis spectra of copper colloid prepared by PLAL of CuO powder in ethyl acetate 2, 4 and 6 hours after the synthesis.

the depicted time period the maximum of the plasmon band shifts from 569 nm to 579 nm. The shift is caused by a partial oxidation of the surface of the nanoparticles. The formation of this thin oxide layer changes the dielectric constant and therefore the plasmon resonance is red shifted.[30]

Transmission electron microscopy of the colloids synthesized by PLAL of CuO powder proves the generation of copper nanoparticles (Figure 2a). As the exemplary Figure 2b

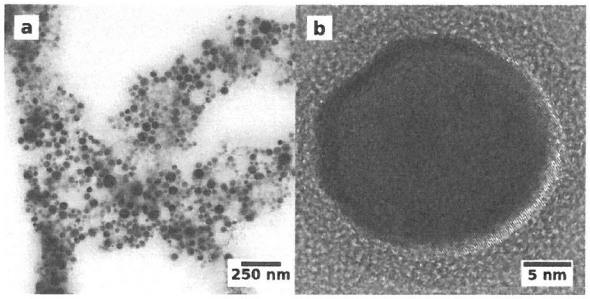

Figure 2: TEM images of Copper nanoparticles synthesized by PLAL of CuO powder in ethyl acetate: (a) TEM image, (b) high resolution TEM image.

depicts the particles are monocrystalline. The evaluation of the size of the nanoparticles reveals a bimodal distribution as shown in Figure 3. There are small irregularly shaped particles with a diameter of (2.7 ± 1.3) nm and bigger spherical particles with a diameter of (21 ± 13) nm.

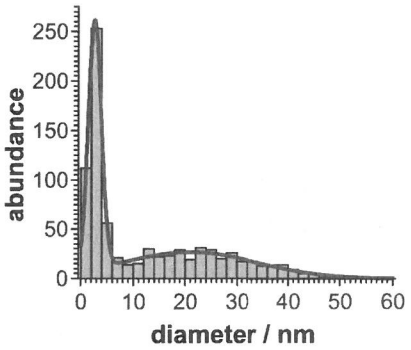

Figure 3: Size distribution of copper nanoparticles generated by PLAL of CuO in ethyl acetate based on 800 particles from 12 TEM images.

In order to understand this size distribution one has to consider that every particle, as soon as it is formed, is hit by the laser pulses several times. Thus the properties of the generated colloids should depend on the number of the ablation pulses. Therefore, the duration for the ablation of CuO suspensions was varied from 1 to 10 min. (1200 to 12000 pulses) and the resulting colloids were characterized by TEM. The amount of small nanoparticles (2.7 nm) proved to be on a high level for any of the investigated ablation durations. In contrast the concentration of the bigger particles (21 nm) strongly depends on the amount of laser pulses. For short ablation times barely any of the bigger particles can be found while they become dominant at longer ablation times. This means that the small particles are not formed by fragmentation of the bigger ones but the bigger nanoparticles are generated by a growth process. Figure 4 depicts the suggested mechanism of the colloid generation by laser ablation of suspensions. During the first step the precursor is ablated and small particles are formed. These primary particles may then aggregate during the ablation. If these aggregates absorb sufficient amounts of laser energy, they form bigger particles by a coalescence process.[27,35] As these secondary particles are nearly perfect spheres, and

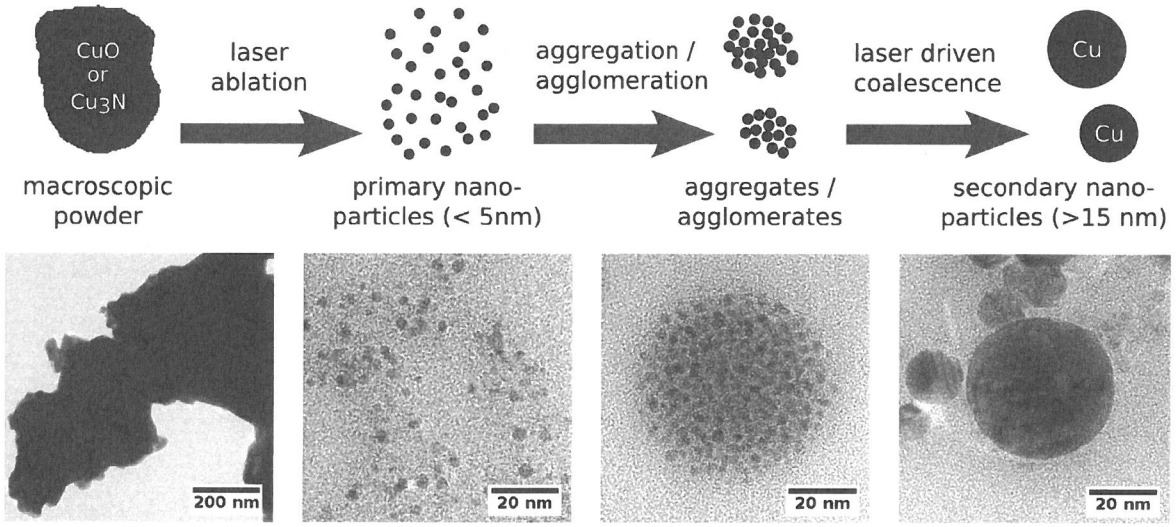

Figure 4: Proposed mechanism for the the generation of copper nanoparticles by PLAL of suspensions. Upper part: schematic of the involved processes; Lower part: corresponding TEM images.

monocrystalline, it can be assumed they were completely molten during their formation.

The particles can be assigned unambiguously to metallic copper by comparing the measured copper EEL spectra (Figure 5) with those in the literature.[32] This is consistent with

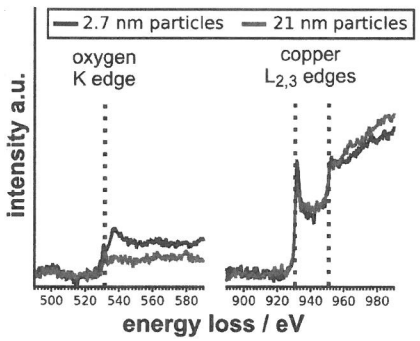

Figure 5: Electron energy loss spectra at the oxygen K (left) and copper $L_{2,3}$ (right) edges of smaller (black) and larger (red) particles generated by PLAL of CuO. The dotted lines mark the edge onsets for oxygen and copper respectively.[36]

the recorded UV-Vis spectra (Figure 1). At a closer look the copper L_3 edge at 930 eV shows a sharp peak. This can be assigned to unoccupied 3d states originating from copper atoms with a higher oxidation state. The weak but distinct feature present at 532 eV (oxygen K

edge) approves the presence of copper oxide. Interestingly, these oxidation features are more pronounced for smaller particles. As the surface to volume ratio is higher for the smaller particles, this behavior may originate from a surface effect which is most likely an oxidation of the particle surfaces. This is also consistent with the observed red shift of the plasmon peak in the UV-Vis spectra.

In summary, the investigation of the chemical composition of the particles generated by laser ablation of CuO shows that (a) a reduction of copper(II) oxide to metallic copper occurs during the laser ablation and (b) the resulting particles may be reoxidized afterwards. This leads to the question whether the oxidation phenomenon is influenced by the oxygen content of the precursor or caused by ambient oxygen. To address this issue, an oxygen free precursor is used as described in the following paragraph.

Copper(I) nitride

The PLAL of Cu_3N in organic liquids, like ethyl acetate, leads to colloidal solutions. These solutions are, in contrast to the colloids obtained from CuO, opaque, suggesting the presence of bigger particles or aggregates. This is corroborated by TEM measurements. As illustrated in Figure 6a the nanoparticles show a much higher polydispersity compared to the particles generated by PLAL of CuO. The carbon selective EFTEM image (Figure 6b) reveals that the copper particles are surrounded by a carbon layer. The particles are supported on a carbon

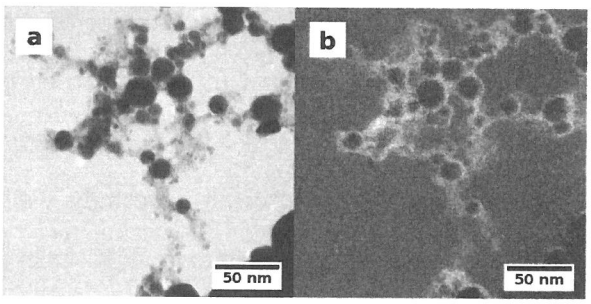

Figure 6: (a) TEM image of Cu_3N particles; (b) EFTEM image at the carbon K edge.

free Si_3N_4 membrane for these measurements. As the copper precursor is not carbon based,

the observed carbon film must emerge from a degradation of the organic solvent during the ablation.

Figure 7 depicts the EEL spectra at the nitrogen K, oxygen K and copper $L_{2,3}$ edge for small (< 5 nm) and larger (> 20 nm) particles. The absence of the nitrogen edge (400 eV) proves that the resulting colloid does not contain fragments of the precursor. The copper is

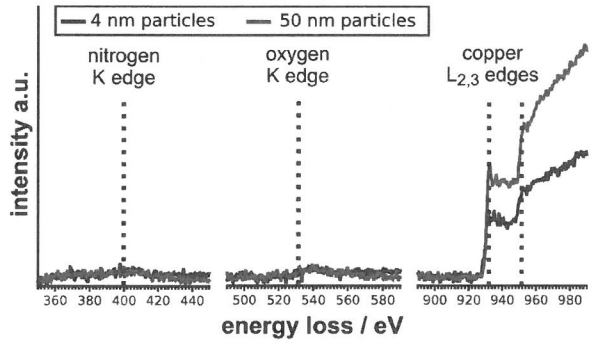

Figure 7: Electron energy loss spectra at the nitrogen K (left), oxygen K (middle), and copper $L_{2,3}$ (right) edges of smaller (black) and larger (red) particles generated by PLAL of Cu_3N. The dotted lines mark the edge onsets for nitrogen, oxygen, and copper respectively.[36]

completely reduced during the ablation. This holds for the small as well as for the larger particles. Considering the proposed mechanism (Figure 4), this leads to the conclusion that the chemical reduction takes place during the formation of the small primary particles. As a consequence, the ablation of powders cannot be treated as a simple fragmentation as it is often suggested in the literature. The changed chemical composition and therefore the different crystal structure hint at a nucleation process even for the generation of the primary particles. In comparison to the CuO precursor Cu_3N leads to copper nanoparticles which show much weaker features of oxidation in the EELS. At the oxygen K edge (532 eV) no signal can be detected and characteristic white lines are only visible for smaller particles and at a much lesser extent than for the CuO precursor. This different behavior of the CuO and Cu_3N precursor indicates that unintended oxidation during the preparation of the TEM samples only plays a minor role. The observed oxidation effects are directly connected to the CuO precursor.

Copper(II)azide

In addition to Cu_3N other nitrogen containing precursors like $Cu(N_3)_2$ can be used successfully for PLAL. Again, TEM images (Figure 8) show small (< 5 nm) and larger particles (> 15 nm). The smaller particles are well separated after short ablation durations, but aggregate when the ablation continues. The larger particles are only formed in significant quantities after at least 1200 laser pulses like it was observed for the preceding precursor materials. Hence, the ablation mechanism is the same as for CuO and Cu_3N (Figure 4). Considering the EELS measurements (Figure 9), the bigger particles are again pure metallic

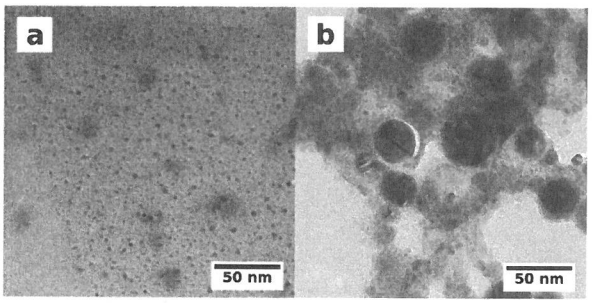

Figure 8: TEM images of copper nanoparticles synthesized by PLAL of $Cu(N_3)_2$ powder in ethyl acetate; (a) 200 laser pulses (b) 6000 pulses.

copper while the smaller particles are partially oxidized. Almost no signal could be found at the nitrogen K edge (400 eV). Thus, the generated particles are again not fragments of the precursor, but formed by nucleation of the decomposed precursor.

While CuO and Cu_3N are stable compounds, $Cu(N_3)_2$ is highly reactive. In fact, even small amounts of energy lead to the decomposition of the $Cu(N_3)_2$. Thus, it enables drastically reduced laser fluences for the PLAL of the suspension, or increases the amount of ablated material for a given laser fluence. An increased amount of ablated material may not necessarily result in a more concentrated colloidal solution, as aggregation and precipitation may occur. In order to address this question, identical experiments with different precursors were performed and at least 3 times reproduced. A fixed amount of the precursor (equivalent to 0.07 mmol copper) was ablated with 1200 pulses. The copper content of the resulting col-

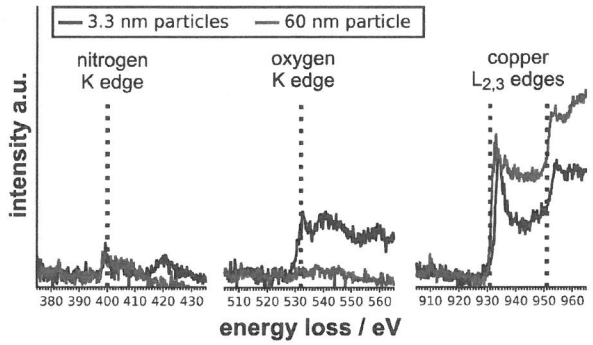

Figure 9: Electron energy loss spectra at the nitrogen K (left), oxygen K (middle), and copper $L_{2,3}$ (right) edges of smaller (black) and larger (red) particles generated by PLAL of $Cu(N_3)_2$. The dotted lines mark the edge onsets for nitrogen, oxygen, and copper respectively.[36]

loids is determined by quantitative flame atomic absorption spectrometry. Figure 10 shows the amount of generated copper nanoparticles relative to the amount of the precursor. As

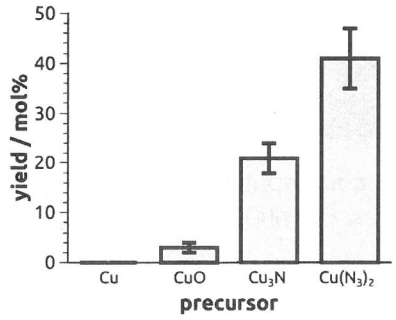

Figure 10: Yield of copper nanoparticles after 1200 laser pulses for different precursors. The calculated yield is based on the amount of copper found (after 1 hour) relative to the amount of used precursor, 0.07 mmol of copper for each material.

mentioned before, the fluence of the unfocused laser is too low to ablate metallic copper. The ablation efficiency is several times higher if Cu_3N is used instead of CuO. This leads to the conclusion that the ablation threshold is significantly lowered in case of the copper nitride. As the threshold is expected to be even lower in the case of $Cu(N_3)_2$, the yield should be considerably increased. Indeed, about 40% of the copper of the precursor can be found in the final colloid. In conclusion, the efficiency of the PLAL of suspensions is correlated with the ablation threshold of the precursor. Thus, a proper choice of the precursor makes high production rates feasible even if the laser fluence is limited.

Copper(I) acetylide

So far, all precursor compounds have in common that gaseous molecules like O_2 and N_2 can be formed. The successful usage of Cu_2C_2 demonstrates that this not a necessary prerequisite. In contrast to the other precursors, metallic copper particles larger than 30 nm are hardly found in the case of Cu_2C_2. Figure 11a shows the resulting particles for the PLAL of Cu_2C_2 in ethyl acetate. The colloid is dominated by particles smaller than 10 nm. The carbon

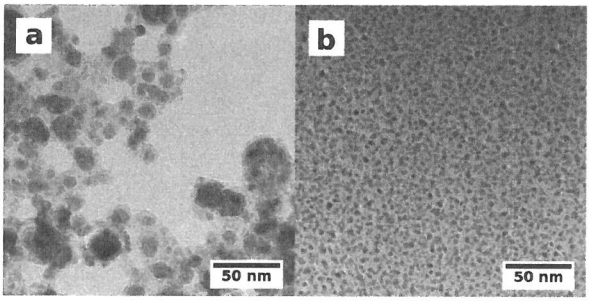

Figure 11: TEM images of copper nanoparticles synthesized by PLAL of Cu_2C_2 powder in (a) ethyl acetate (b) acetonitrile.

liberated during the decomposition can not escape as a gas as it is the case for oxygen and nitrogen. Instead, the carbon forms a shell around the generated nanoparticles. This carbon shell may hinder the aggregation and coalescence processes observed for CuO and Cu_3N precursors (Figure 4). Thus, the formation of larger particles is less probable. This effect is even more pronounced if acetonitrile is used as a solvent (Figure 11b). Here, large amounts of small, well separated nanoparticles with a narrow size distribution of (2.7 ± 0.6) nm are found. In addition, these colloids exhibit an unexpected good colloidal stability for several month. Hence, the carbon of the Cu_2C_2 precursor acts as a stabilizer. Small amounts of carbon on the surface of the particles may be found for every precursor due to solvent degeneration. But the carbon EELS measurements (Figure 12) prove that in the case of the Cu_2C_2 precursor the amount of carbon clearly exceeds these effects. The copper EELS shows only minor oxidation features. Most probably these are caused by reoxidation by ambient oxygen after the synthesis. The vast amount of copper has the oxidation state zero. This is

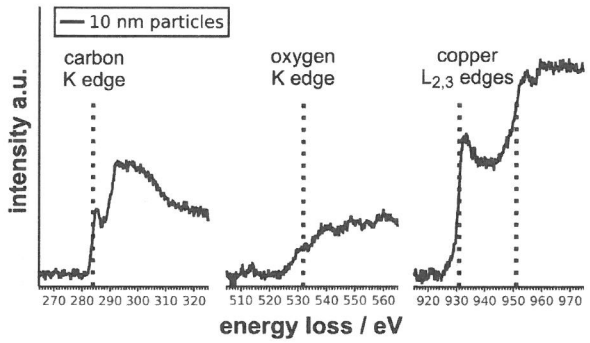

Figure 12: Electron energy loss spectra at the carbon K (left), oxygen K (middle), and copper $L_{2,3}$ (right) edges of particles generated by PLAL of Cu_2C_2. The carbon EELS was recorded while the samples where suspended on a silicon nitride membrane. The dotted lines mark the edge onsets for carbon, oxygen, and copper respectively.[36]

consistent with EFTEM measurements showing copper cores and carbon shells. The absence of distinct white lines in the copper EELS, even for the smallest particles, proves that the change in the chemical composition takes place at the first step of the mechanism.

The investigations on the laser ablation of Cu_2C_2 offers the possibility to control the properties of the generated nanoparticles by varying the chemical composition of the precursor. It also shows the importance of a detailed mechanistic understanding of the physical and chemical processes during the laser ablation.

Conclusion

The pulsed laser ablation of suspensions of copper compounds proves to be an efficient route for the production of metallic copper colloids. We complemented the known ablation of CuO suspended in organic liquids by the usage of several additional precursors. The formation mechanism of nanoparticles by laser ablation of suspensions turned out to be more complex than a simple laser induced fragmentation model. For the setup discussed in this work the following mechanism applies: The μm sized precursor powder is ablated and nanoparticles with a diameter of 1.5 - 4 nm are generated. These primary particles then may aggregate. By the repeated impact of the laser the aggregated particles melt and form secondary particles

by coalescence. These secondary particles are spherical, single crystalline and exhibit a broad size distribution from about 15 nm to several hundred nm. Remarkably, the ablation of CuO leads to pure metallic nanoparticles. Although this change in the chemical composition has a major impact on the properties of the generated nanoparticles, it is often only briefly discussed in the literature. We addressed this question by the usage of the oxygen-free precursor Cu_3N. Electron energy loss spectra of the resulting primary particles proved that the reduction takes place during the first step of the mechanism ruling out the concept of a simple fragmentation. The ablation of suspended $Cu(N_3)_2$ powder leads to copper colloids similar to those obtained from Cu_3N. The usage of the highly reactive $Cu(N_3)_2$ enables significant higher production rates. The ablation of Cu_2C_2 leads to stable colloidal solutions mainly consisting of the small primary particles. This is caused by the fact that in contrast to the other precursors the carbon can not be liberated as a gas. It prevents the aggregation of the primary particles and therefore stops the presented mechanism after the first step. The proper choice of the precursor for the laser ablation of suspensions not only provides insight in the mechanism but also gives the opportunity to design the properties of the resulting colloids. The results of the presented work leaves us with an optimistic perspective that on the one hand further copper precursors and on the other hand precursors for other metals may be developed in the future. An efficient and targeted development of suitable precursors will make the laser ablation of suspensions a versatile and universal method for the synthesis of colloidal solutions.

Acknowledgement

The authors like to thank Yeliz Akyürek and Michael W. Linscheid for the flame atomic absorption spectrometry measurements.

References

(1) Xia, T.; Malasarn, D.; Lin, S.; Ji, Z.; Zhang, H.; Miller, R. J.; Keller, A. A.; Nisbet, R. M.; Harthorn, B. H.; Godwin, H. A.; Lenihan, H. S.; Liu, R.; Gardea-Torresdey, J.; Cohen, Y.; Mädler, L.; Holden, P. A.; Zink, J. I.; Nel, A. E. Implementation of a Multidisciplinary Approach to Solve Complex Nano EHS Problems by the UC Center for the Environmental Implications of Nanotechnology. *Small* **2013,** *9* (9-10), 1428-1443.

(2) Turkevich, J.; Stevenson, P. C.; Hillier, J. A study of the nucleation and growth processes in the synthesis of colloidal gold. *Discuss. Faraday Soc.* **1951,** *11,* 55-75.

(3) Brust, M.; Walker, M.; Bethell, D.; Schiffrin, D. J.; Whyman, R. Synthesis of thiol-derivatised gold nanoparticles in a two-phase Liquid-Liquid system. *J. Chem. Soc., Chem. Commun.* **1994,** No. 7, 801-802.

(4) Barcikowski, S.; Hahn, A.; Kabashin, A. V.; Chichkov, B. N. Properties of nanoparticles generated during femtosecond laser machining in air and water. *Appl. Phys. A* **2007,** *87* (1), 47-55.

(5) Albrecht, M. A.; Evans, C. W.; Raston, C. L. Green chemistry and the health implications of nanoparticles. *Green Chem.* **2006,** *8* (5), 417-432.

(6) Pustovalov, V. K.; Smetannikov, A. S.; Zharov, V. P. Photothermal and accompanied phenomena of selective nanophotothermolysis with gold nanoparticles and laser pulses. *Laser Phys. Lett.* **2008,** *5* (11), 775-792.

(7) Lin, F.; Yang, J.; Lu, S.-H.; Niu, K.-Y.; Liu, Y.; Sun, J.; Du, X.-W. Laser synthesis of gold/oxide nanocomposites. *J. Mater. Chem.* **2010,** *20* (6), 1103-1106.

(8) Wagener, P.; Schwenke, A.; Barcikowski, S. How citrate ligands affect nanoparticle adsorption to microparticle supports. *Langmuir* **2012,** *28* (14), 6132-6140.

(9) Minnich, A. J.; Dresselhaus, M. S.; Ren, Z. F.; Chen, G. Bulk nanostructured thermoelectric materials: current research and future prospects. *Energy Environ. Sci.* **2009,** *2* (5), 466-479.

(10) Henglein, A. Physicochemical Properties of Small Metal Particles in Solution: "Microelectrode" Reactions, Chemisorption, Composite Metal Particles, and the Atom-to-Metal Transition. *J. Phys. Chem. B* **1993,** *97* (21), 5457-5471.

(11) Kazakevich, P.; Simakin, A.; Voronov, V.; Shafeev, G. Laser induced synthesis of nanoparticles in liquids. *Appl. Surf. Sci.* **2006,** *252* (13), 4373-4380.

(12) Barcikowski, S.; Compagnini, G. Advanced nanoparticle generation and excitation by lasers in liquids. *Phys. Chem. Chem. Phys.* **2013,** *15* (9), 3022-3026.

(13) Zeng, H.; Du, X.-W.; Singh, S. C.; Kulinich, S. A.; Yang, S.; He, J.; Cai, W. Nanomaterials via Laser Ablation/Irradiation in Liquid: A Review. *Adv. Funct. Mater.* **2012,** *22* (7), 1333-1353.

(14) Golightly, J. S.; Castleman, A. W. Analysis of Titanium Nanoparticles Created by Laser Irradiation under Liquid Environments. *J. Phys. Chem. B* **2006,** *110* (40), 19979-19984.

(15) Izgaliev, A. T.; Simakin, A. V.; Shafeev, G. A.; Bozon-Verduraz, F. Intermediate phase upon alloying Au-Ag nanoparticles under laser exposure of the mixture of individual colloids. *Chem. Phys. Lett.* **2004,** *390* (4-6), 467-471.

(16) Yeh, M.-S.; Yang, Y.-S.; Lee, Y.-P.; Lee, H.-F.; Yeh, Y.-H.; Yeh, C.-S. Formation and Characteristics of Cu Colloids from CuO Powder by Laser Irradiation in 2-Propanol. *J. Phys. Chem. B* **1999,** *103* (33), 6851-6857.

(17) Kawasaki, M. Laser-Induced Fragmentative Decomposition of Fine CuO Powder in

Acetone as Highly Productive Pathway to Cu and Cu_2O Nanoparticles. *J. Phys. Chem. C* **2011,** *115* (12), 5165-5173.

(18) Kawasaki, M.; Nishimura, N. 1064-nm laser fragmentation of thin Au and Ag flakes in acetone for highly productive pathway to stable metal nanoparticles. *Appl. Surf. Sci.* **2006,** *253* (4), 2208-2216.

(19) Kosalathip, V.; Dauscher, A.; Lenoir, B.; Migot, S.; Kumpeerapun, T. Preparation of conventional thermoelectric nanopowders by pulsed laser fracture in water: application to the fabrication of a pn hetero-junction. *Appl. Phys. A* **2008,** *93* (1), 235-240.

(20) Chubilleau, C.; Lenoir, B.; Migot, S.; Dauscher, A. Laser fragmentation in liquid medium: A new way for the synthesis of PbTe nanoparticles. *J. Colloid Interface Sci.* **2011,** *357* (1), 13-17.

(21) von der Linde, D.; Sokolowski-Tinten, K.; Bialkowski, J. Laser-solid interaction in the femtosecond time regime. *Appl. Surf. Sci.* **1997,** *109-110,* 1-10.

(22) Miotello, A.; Kelly, R. Laser-induced phase explosion: new physical problems when a condensed phase approaches the thermodynamic critical temperature. *Appl. Phys. A* **1999,** *69* (7), S67-S73.

(23) Wagener, P.; Ibrahimkutty, S.; Menzel, A.; Plech, A.; Barcikowski, S. Dynamics of silver nanoparticle formation and agglomeration inside the cavitation bubble after pulsed laser ablation in liquid. *Phys. Chem. Chem. Phys.* **2013,** *15* (9), 3068-3074.

(24) Takami, A.; Kurita, H.; Koda, S. Laser-Induced Size Reduction of Noble Metal Particles. *J. Phys. Chem. B* **1999,** *103* (8), 1226-1232.

(25) Werner, D.; Furube, A.; Okamoto, T.; Hashimoto, S. Femtosecond Laser-Induced Size Reduction of Aqueous Gold Nanoparticles: In Situ and Pump-Probe Spectroscopy

Investigations Revealing Coulomb Explosion. *J. Phys. Chem. C* **2011,** *115* (12), 8503-8512.

(26) Plech, A.; Kotaidis, V.; Lorenc, M.; Boneberg, J. Femtosecond laser near-field ablation from gold nanoparticles. *Nat. Phys.* **2005,** *2* (1), 44-47.

(27) Boyer, P.; Meunier, M. Modeling Solvent Influence on Growth Mechanism of Nanoparticles (Au, Co) Synthesized by Surfactant Free Laser Processes. *J. Phys. Chem. C* **2012,** *116* (14), 8014-8019.

(28) Kawasaki, M.; Nishimura, N. Laser-Induced Fragmentative Decomposition of Ketone-Suspended Ag_2O Micropowders to Novel Self-Stabilized Ag Nanoparticles. *J. Phys. Chem. C* **2008,** *112* (40), 15647-15655.

(29) Amendola, V.; Meneghetti, M. What controls the composition and the structure of nanomaterials generated by laser ablation in liquid solution? *Phys. Chem. Chem. Phys.* **2013,** *15* (9), 3027-3046.

(30) Rice, K. P.; Walker, E. J.; Stoykovich, M. P.; Saunders, A. E. Solvent-Dependent Surface Plasmon Response and Oxidation of Copper Nanocrystals. *J. Phys. Chem. C* **2011,** *115* (12), 1793-1799.

(31) Leapman, R. D.; Grunes, L. A.; Fejes, P. L. Study of the L_{23} edges in the 3d transition metals and their oxides by electron-energy-loss spectroscopy with comparisons to theory. *Phys. Rev. B* **1982,** *26* (1), 614-635.

(32) Shindo, D.; Hiraga, K.; Tsai, A.-P.; Chiba, A. Cu $L_{2,3}$ White Lines of Cu Compounds Studied by Electron Energy Loss Spectroscopy. *J. Electron Microsc.* **1993,** *42* (1), 48-50.

(33) Straumanis, M.; Cīrulis, A. Das Kupfer(II)-azid Darstellungsmethoden, Bildung und Eigenschaften. *Z. Anorg. Allg. Chem.* **1943,** *251* (4), 315-331.

(34) Heil, T.; Kohl, H. Optimization of EFTEM image acquisition by using elastically filtered images for drift correction. *Ultramicroscopy* **2010,** *110* (7), 748-753.

(35) Tsuji, T.; Yahata, T.; Yasutomo, M.; Igawa, K.; Tsuji, M.; Ishikawa, Y.; Koshizaki, N. Preparation and investigation of the formation mechanism of submicron-sized spherical particles of gold using laser ablation and laser irradiation in liquids. *Phys. Chem. Chem. Phys.* **2013,** *15* (9), 3099-3107.

(36) Egerton, R. F. *Electron Energy-Loss Spectroscopy in the Electron Microscope,* 3rd ed.; Springer: New York, Dordrecht, Heidelberg, London, 2011; p 424.

Graphical TOC Entry